Transmembrane Helix Stability: The Effect of Helix-Helix Interactions Studied by Fourier Transform Infrared Spectroscopy

James Sturgis,* Bruno Robert,* and Erik Goormaghtigh#

*Section de Biophysique des protéines et des Membranes DBCM/CEA and URA 2096/CNRS, Centre d'études de Saclay, 91191 Gif sur Yvette CEDEX, France, and #Laboratoire de Chimie physique des Macromolécules aux interfaces, CP206/2 Université Libre de Bruxelles, B-1050 Brussels, Belgium

ABSTRACT We have measured, using infrared spectroscopy, the hydrogen/deuterium exchange rates of the amide protons in the photosynthetic antenna of *Rhodospirillum rubrum*. These measurements were made not only on the intact protein in detergent solution but also on two dissociated forms (B820 and B777). We have, on the basis of our knowledge of the structure of this protein, been able to assign the various groups of amide protons that exchange with different time constants to distinct regions of the protein. The most protected group of protons that we observe exchanging with time constants near 6000 min we assign to the transmembrane helices. The slow exchange rates measured for the amide protons of the transmembrane helices of this protein in detergent solution may indicate a destabilization of the helices in detergent solution compared with the membrane. This group of protons is progressively destabilized by stepwise dissociation of the antenna protein, and this destabilization is greater than we can account for by increases in solvent accessibility. We suggest that the observed loss of amide proton protection in the transmembrane helices as they are dissociated might be due to an increase in the helix flexibility and breathing motions as interactions between helices are reduced.

INTRODUCTION

The classical method for measuring amide proton/deuteron exchange is NMR (Englander and Mayne, 1993). In its most recent incarnations the usual approach is to measure changes in amide proton protection as a protein refolds. This can now be done with impressive resolution both in time (1 ms) and space (individual amide protons). Unfortunately the use of NMR methods is restricted to systems in which various criteria are met. The protein must be soluble at the high concentrations needed for NMR in a nonviscous solvent, and the protein must tumble rapidly. This effectively restricts studies to small monomeric water soluble proteins available in relatively large amounts. Recently, two techniques have been developed that allow measurements of amide proton exchange in samples ill adapted to NMR measurements, mass spectrometry and Fourier transform infrared spectroscopy (FTIR), which we use in this paper.

Hydrogen/deuterium exchange measurements by FTIR have previously been used to study a number of integral membrane proteins in various lipid environments. These studies have as a rule demonstrated a proportion of amide protons undergoing almost no exchange, which are assigned to transmembrane helical regions. For example, in the study by Earnest et al. (1990) of bacteriorhodopsin in purple membranes, 70–75% of the amide protons were resistant to exchange. This value roughly corresponds to the membrane-embedded part of the protein. A more recent study of phospholamban (Ludlam et al., 1996) again indicated a large proportion of amide protons that were not exchanging and provided evidence that these were associated with the transmembrane helical region, whereas faster exchanging amide protons were associated with the cytoplasmic domain. Notable exceptions to the rule of little exchange of amide protons in transmembrane helices are the studies of the glucose transporter by Alvarez et al. (1987) and the CHIP28 protein by Haris et al. (1995) in which in each case almost all the amide protons exchanged very rapidly. This was attributed to high water accessibility to the interior, membrane-spanning portion of the protein via the presumed pore. This study differs in addition from those sited above in that the protein was extracted in *N*-lauryl sarcosine rather than reconstituted into phospholipid vesicles in the case of phospholamban or in a native paracrystaline membrane for bacteriorhodopsin. The difference in the lipid environment could be important in that it is at least possible that in the nonexchanging systems the lipid was in a gel rather than fluid phase. The $P_{\beta'}$ L_{α} phase transition of dimyristoylphosphatidyl choline, used in the measurements of phospholamban made at room temperature, is close to room temperature (Janiak et al., 1979). Similarly, at ambient temperatures the purple membrane is in the gel phase (Ashikawa et al., 1994).

The core antenna of the photosynthetic bacterium *R. rubrum* provides an ideal model for investigating factors that affect the stability and structure of transmembrane helices. This protein is reasonably well characterized structurally (Karrasch et al., 1995) (see below) and can be prepared either intact or in various degrees of dissociation (Loach et al., 1985; Sturgis and Robert, 1994). The dissociation of this protein by the detergent *n*-octyl-β-D-glucopyranoside results in the accumulation of an intermediate subunit form called B820 at lower detergent concentrations

Received for publication August 11, 1997 and in final form November 6, 1997.

Address reprint requests to Dr. James N. Sturgis, SBPM/DBCM, CE de Saclay, 91191 Gif sur Yvette CEDEX, France. Tel.:33-01-69-08-90-15; Fax: 33-01-69-08-43-89; E-mail: james@eliager.saclay.cea.fr.

0006-3495/98/02/988/07 $2.00

than are necessary for the complete dissociation into a form called B777 containing individual polypeptides with their associated pigment molecules (Sturgis and Robert, 1994). The structural knowledge coupled with the ability to prepare the protein in various different aggregation states makes this protein an ideal sample for hydrogen/deuterium (H/D) exchange measurement using FTIR.

In this paper we present the first measurements of H/D exchange rates in transmembrane helices in both an intact isolated membrane protein and in various subunit forms of the same protein. These measurements are interpreted in the light of our current structural knowledge of these proteins in which they allow the assignment of different exchange rates to different structural regions of the protein.

MATERIALS AND METHODS

R. rubrum core antenna (B873) was purified from washed, reaction center-depleted chromatophores (Cogdell et al., 1982) of the carotenoidless strain $G9^+$, as previously described (Sturgis and Robert, 1994). Purified antenna protein was dialyzed against 1 mM Tris-HCl, pH 8.0, buffer to reduce the buffer ion and detergent concentrations, and this sample was used for the acquisition of the B873 data. The two subunit forms of the antenna, B820 and B777, were prepared by incubation of the dialyzed-purified core antenna with an appropriate amount of *n*-octyl-β-D-glucopyranoside sufficient to convert the B873 preparation into the desired spectral from. For FTIR measurements, films containing approximately 100 μg of protein were prepared by permitting the sample to dry on a germanium attenuated total reflection (ATR) plate (50 $\times$ 20 $\times$ 2 mm) by slow solvent evaporation. The absorption spectra of films prepared similarly by drying the same solutions on quartz plates were taken to ensure the samples retained the expected spectral form.

Spectra were recorded on a Bruker IFS55 spectrophotometer, and the internal reflection element was the germanium plate, described above, coated with the sample with an aperture angle of 45° yielding 25 internal reflections. H/D exchange was initiated by connecting the sample holder to a flow of D_2O saturated nitrogen. Then for each time point, 16 scans were recorded and averaged with a resolution of 4 cm^{-1}, as described in Raussens et al. (1996).

After acquisition, the spectra were corrected for the contributions of both atmospheric water (Goormaghtigh and Ruysschaert, 1994) and lateral side chains (Goormaghtigh et al., 1994a) to the spectra. For kinetic analyses, the amide I and amide II bands were integrated numerically between 1590 and 1710 cm^{-1} and between 1500 and 1575 cm^{-1}, respectively. The intensities of the amide II band were normalized to those of the amide I band to compensate for changes in the protein film thickness due to adsorption of D_2O. Then the data were scaled to give an initial signal before exchange of 100. Laplace transforms of the kinetic data were calculated using the method of Provencher (1982), assuming at the end-point no contribution from the amide II band. This assumption seems reasonable on the basis of the absence of an amide II band in the FTIR spectra of antenna protein samples in which H/D exchange has continued over a period of several weeks (Gall, Sturgis, and Robert, personal communication).

RESULTS

In Fig. 1, we show how the ATR-FTIR absorption spectra change with time after initiation of the hydrogen deuterium exchange. In these spectra, there are three major bands derived from the peptide backbone: the amide I band centered near 1650 cm^{-1}, the amide II band near 1550 cm^{-1}, and the amide II′ band near 1460 cm^{-1}. The amide I band

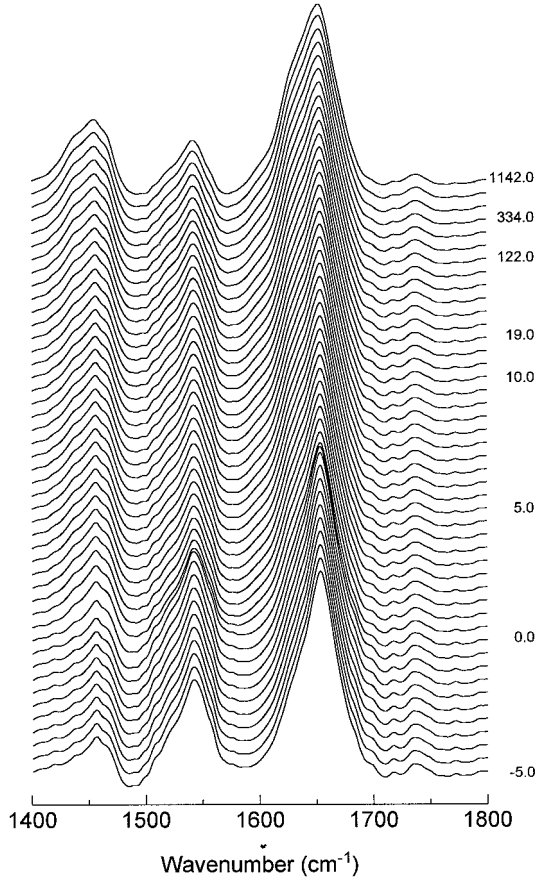

FIGURE 1 Time-dependent spectra for B873, obtained as described in Materials and Methods from an essentially detergent-free antenna preparation, were obtained at various times after the initiation of H/D exchange. Spectra were obtained at 30-s intervals from −5 min to 10 min and thereafter at 11.5, 14, 19, 27.4, 40.3, 59.1, 85.7, 122, 173, 242, 334, 459, 625, 847, and 1142 min relative to the initiation of exchange. Certain spectra are labeled with the time in minutes. The spectra shown are those attributed to the polypeptide chain obtained after removal of contributions due to atmospheric water and side chain contributions, as described in the text.

is due mainly to CO stretching with some contributions from CN stretching and is sensitive to the protein secondary structure. Indeed, the shape of this band can be used to estimate protein secondary structure (Goormaghtigh et al., 1994b for review). The amide II band derives from in-plane NH bending coupled to the CN stretching of the peptide bond. As can be readily observed, the intensity of this band decreases markedly during exchange. Those peptide bonds in which the proton is exchanged for a deuteron no longer contribute to this band but rather to the in-plane ND bending band, which appears near 1000 cm^{-1}. The CN stretching contribution moves to 1450 cm^{-1} in which it mixes with other backbone modes to give the amide II′ band. The amide II′ band is thus responsible for the increase in absorption during the experiment and is clearly observable in the 1460 cm^{-1} region.

Measurements of the time dependence of the infrared absorption spectrum after starting deuterium exchange were

equally made on the two subunit forms of the *R. rubrum* antenna complex (B820 and B777). The shape of the amide I bands observed in each of the three samples we examined were all very similar and entirely consistent with our previous conclusions of little or no variation of helical content with dissociation of the intact antenna to the subunit forms (Sturgis and Robert, 1994). For all samples, we verified that thin films prepared similarly to those for infrared spectroscopy, but on quartz rather than germanium plates, remained in the appropriate spectral form.

In Fig. 2, we show the observed development in the area of the amide II band with time for the three different forms of the antenna protein studied. In panel A, we show a portion of the data with a linear time scale, and in panel B, we show the data with a logarithmic time scale in order to give a pseudo-linear representation. From the data in panel A, it can be seen (especially in the intact system) that there are a portion of the amide hydrogens that exchange rapidly over a few minutes and then others that exchange much more slowly. From a comparison of the different forms of the protein, it is clear that the dissociation by detergent has a profound effect on the kinetics of deuterium exchange. Qualitatively, these seem to be a reduction in the fast rates of exchange on one hand and an acceleration of the slower rates of exchange. In order to perform a more quantitative analysis of the data, it is necessary to obtain some idea of the various rate constants involved.

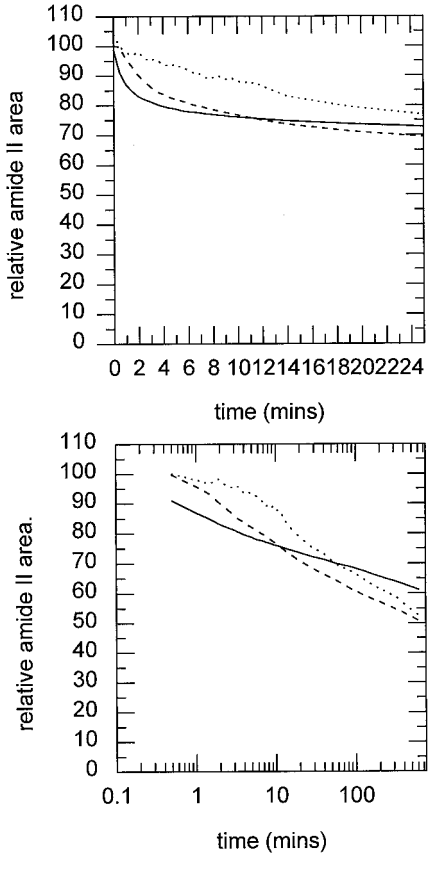

FIGURE 2 Normalized amide II contributions as a function of time. *Upper panel*, linear scales; *lower panel*, logarithmic time scale. Each point represents the integrated area of the amide II band in spectra like those in Fig. 1 after the given time for H/D exchange relative to an initial area of 100 before the start of the exchange. Data from three different states of the antenna protein, prepared as described in Materials and Methods, are shown: *solid line*, B873; *dashed line*, B820; *dotted line*, B777.

The kinetics that we show here result from many individual amide protons, including one for each of the 101 peptide bonds, each of which is expected to have its own characteristic first order exchange rate under the conditions used. Though we do not have sufficient data or resolution to assign 101 rate constants, it is possible to obtain an idea of the distribution of rate constants from the Laplace transform of the time-dependent exchange data (Goormaghtigh et al., 1994a). In Fig. 3 are shown the Laplace transforms of the data shown in Fig. 2. In this method the figure shows the envelope of the rate constant distribution. This analysis method is somewhat prone to instability when applied to noisy data; however the transforms that we obtained were reasonably stable and form a self consistent set. For the intact complex we observe five groups of rate constants for the exchange, and ~65% of the amide hydrogens exchange slowly with time constants of ~6000 min, whereas the remaining 35% of amide protons are divided into four groups of approximately equivalent size (7–10%) with time constants near 100, 10, 2, and 0.5 min. It should be remarked that this last group of quickly exchanging protons exchange is within the maximum resolution of the measurements, and thus 0.5 min is simply a lower limit for this time constant.

Comparison of the transforms for data from the three different structural forms allows us to quantify the effects of detergent induced dissociation on the exchange rates. In the intermediate form (B820) there are three changes in the distribution of exchange rates. First, the slow exchange rates are slightly accelerated from 1.6×10^{-4} min^{-1} to 5×10^{-4} min^{-1}. Second, the two fastest series of exchange rates

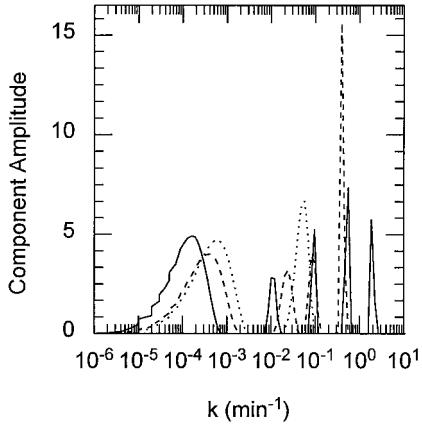

FIGURE 3 Laplace transform of the data in Fig. 2 showing the distribution of rate constants. The transformed data was normalized to an integrated area of 100. *Solid line*, B873; *dashed line*, B820; *dotted line*, B777.

appear to merge to give a single group of hydrogens with a time constant of 2.2 min. Finally, the group initially exchanging with a time constant of about 100 min, now exchange with a time constant nearer 40 min. Remarkably the H/D exchange rate of those peptide bonds that initially gave a rate of $\sim 0.1\ min^{-1}$ appear to be virtually unaffected by the dissociation. In the fully dissociated form (B777), the various changes in the rate constants progress. Notably the slowly exchanging protons, which continue to represent ~65% of the total, now exchange still faster with a time constant of ~1000 min; whereas the remainder of the protons now all exchange as a single group with a time constant of ~20 min.

DISCUSSION

It is of interest to consider the results for the accessibility of the various amide hydrogens to deuterium exchange with reference to the protein structure. Though there is no high resolution structure of the protein used here either in its native conformation or in the two subunit forms investigated, a certain amount of structural detail can be inferred by combining information from the high resolution structures of a number of closely related proteins (McDermott et al., 1995; Koepke et al., 1996), the low resolution structure of the protein we have used in the present study (Karrasch et al., 1995), various spectroscopic studies of this and closely related proteins (Sturgis et al., 1997, Olsen et al., 1997), and the structural relationship between the various subunit forms (Sturgis and Robert, 1994; 1995).

Protein structure

The basic building block of the core antenna protein we have studied here is a heterodimeric subunit containing two polypeptides (α and β) of 52 and 54 amino acids, respectively and two bacteriochlorophyll *a* molecules illustrated in Fig. 4. Each of the two polypeptides contains three regions:

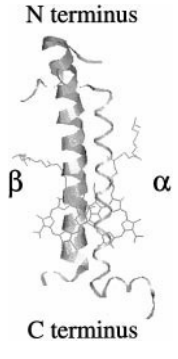

FIGURE 4 Schematic diagram of the structure of the heterodimeric subunit of the antenna protein discussed in the text. The diagram shows the heterodimeric subunit with the α- (*right*) and β- (*left*) polypeptides sandwiching 2 Bchl a cofactor molecules. This structure shown is based on the work of Karrasch et al. (1995), McDermott et al. (1995), and Koepke et al. (1996).

an N-terminal cytoplasmic region, a transmembrane α-helical region, and a C-terminal periplasmic domain. Within the transmembrane region of each polypeptide, the Nϵ atom of a histidyl residue acts as a ligand to the central magnesium of a bacteriochlorophyll molecule. Each polypeptide also provides a ligand to the C_2 acetyl group of the bacteriochlorophyll molecule that it binds from the C-terminal region, and it is believed that the Nδ hydrogen of the liganding histidines interact with the C_9 ketone group of the other bacteriochlorophyll molecule (Olsen et al., 1997; Hu et al., 1997) so stabilizing the dimer. The β-polypeptide probably contains an irregularly structured short N-terminal region of residues 1–10, followed by a long transmembrane helix from residue 11–44 nearly perpendicular to the membrane, a short turn to bring tryptophan 46 within hydrogen bonding distance of the bacteriochlorophyll acetyl group, and an irregularly structured C-terminal region for residues 47–54. The structure of the α-polypeptide is perhaps less well defined in the N-terminal region since it is unclear exactly where the transmembrane helical region should start. However after an initial segment, possibly in a 3_{10} helical structure, the transmembrane helix runs from about residue 8–35. Then after a turn, there is an amphipathic helix from about residues 37–49. The transmembrane helix is very close to perpendicular to the membrane plane, whereas the amphipathic helix probably lies along the membrane surface and includes tryptophan 39, which ligands the second bacteriochlorophyll acetyl group. From comparison with the known structures, we can be reasonably certain of the structures within the membrane and in the C-terminal region as the protein we have studied has strong homology in this region with that investigated by Koepke et al. (1996). However, the accuracy of the description in the N-terminal regions is less certain. The angle of the C-terminal amphipathic helix to the membrane surface deserves comment because although helix is nearly parallel to the membrane in the *Rhodopseudomonas acidophila* LH2 structure (McDermott et al., 1995), it is at a considerable angle in the *R. molischianum* structure of Koepke et al. (1996). However, in this structure this region is involved in a number of crystallographic contacts and is possibly orientated in the membrane more or less parallel to the membrane surface, as observed in the *R. acidophila* LH2 structure.

The native antenna protein (B873) is formed from a cyclic oligomer containing 16 repetitions of this heterodimeric subunit (Karrasch et al., 1995). This cyclic oligomerization involves the creation of and is stabilized by a number of contacts among adjacent subunits. In particular, there are close contacts between the pigment molecules in adjacent helices. The transmembrane helices probably pack together reasonably well. In addition, there are a few possible hydrogen bonds between subunits in the N- and C-terminal regions between the α-polypeptide of one subunit and the β-polypeptide of the next subunit in the ring (Koepke et al., 1996).

The intermediate form (B820) is believed to be composed of a head to tail dimer of the basic heterodimer (Sturgis and

Robert, 1995) and thus contains four polypeptides and pigments. Though it is not immediately clear how the two heterodimers are arranged on the basis of the spectral properties that place the chromophore pairs far apart, it seems probable that the interaction involves the N-terminal regions. Finally, the dissociated form studied here is thought to represent isolated polypeptides with bound pigment molecules (Sturgis and Robert, 1994). Most importantly, the secondary structure composition remains almost completely unaffected by the dissociation as observed by infrared spectroscopy (Sturgis and Robert, 1994; and this work) and in agreement with earlier far ultraviolet CD spectroscopy (Chang et al., 1990). This dissociated form therefore represents the structurally stable helical units proposed as the intermediate state in the folding of helical membrane proteins (Popot and Engelman, 1990) with each containing a bound pigment molecule.

H/D exchange rates in different parts of the structure

The major group of slowly exchanging protons, which in each form studied represents ~64% (63.8 ± 3.1) of the peptide bonds, were assigned to the transmembrane helical regions. The regions assigned to the transmembrane segments represent ~60% of the amide nitrogens in the structure. Based on the description above, this corresponds well with the size of the signal from the slowly exchanging protons. The slight underestimation might indicate that the α-polypeptide transmembrane helix extends slightly further toward the N terminus than proposed above. Of course, possible differences in extinction coefficient among the various amide groups cannot be ignored (de Jongh et al., 1996).

The assignment and understanding of the changes in the exchange rates of the other groups of protons is more complex. We believe there are two possible effects. One effect is a reduction in the effective kinetic resolution due to the presence of relatively large amounts of detergent in the two dissociated samples (B820 and B777). In addition to this effect, we would propose a progressive dissociation-induced, or detergent-induced, destabilization of those 8–10 protons that initially had exchange rates near 0.01 min^{-1} and a remarkable insensitivity of the similar number of protons with exchange rates near 0.1 min^{-1} to dissociation. The mechanism whereby the detergent could reduce the effective kinetic resolution is unclear. One possibility is that the high concentrations of hydroscopic detergent slow the equilibration of the deuterium oxide vapor across the increasingly thick and hydrated protein/detergent film resulting in a merging of all the exchanging groups faster than 2.2 min in the B820 form and about 14 min in the B777 form. This effect would thus progressively amalgamate the groups of faster exchanging protons and reduce their apparent exchange rate without necessarily stabilizing the structure. Alternatively the loss of kinetic resolution might be due to stabilization of certain regions of the protein in the viscous detergent-rich environment. It should be recalled that the effect is unlikely to be due to the detergent acting as a barrier to D_2O diffusion as even phospholipids are ineffective as such a barrier (Goormaghtigh et al., 1994a)

It is hard to assign the various groups of more quickly exchanging protons, however the group that is progressively destabilized by dissociation may well represent the peptide bonds in the C-terminal helical region of the α-polypeptide. This assignment is justified because this segment is expected to be well structured from the known three-dimensional structures, thus showing a low exchange rate in the native form, and to change its environment substantially during dissociation both as it is expected to be involved in intersubunit contacts and is involved in interactions with the pigment molecules, which are known to be perturbed by dissociation (Sturgis and Robert, 1994). This would leave the peptide bonds of the termini of the β-polypeptide, the N terminus of the α-polypeptide, and the various loops and turns to be assigned. It seems possible that the most stable remaining group of peptide bonds, with an exchange time constant of about 10 min insensitive to the dissociation, are associated with one of the N-terminal regions perhaps of the β-polypeptide, however any such assignment must remain highly tentative.

As we assign the different regions of the protein to different exchange rate ranges above, it appears that the different aggregation states we examined differ in the exchange rates for amide groups within the transmembrane helical segments. Thus, we observe a rate of exchange six times faster in the fully dissociated (B777) form than in the native (B873) form. It is probable that this difference results, to a large extent, from changes in helix accessibility to deuterium oxide as the forms differ in the presumed exposure of the helices. For example, we estimate the relative solvent accessible areas for the transmembrane helices in the different forms to be ~75% in the fully dissociated (B777) form, ~60% in the intermediate (B820) form, and ~25% in the native (B873) form. However, these values must overestimate the accessibility as the detergent will to some extent restrict D_2O access. In addition to changes in the solvent accessibility, the exchange rate acceleration in the dissociated forms reflects differences in the stability of the transmembrane helices. Our results would appear to suggest that this effect is relatively restricted, thus providing evidence that the detergent environment does not seriously perturb the stability of the helical secondary structure of the transmembrane regions. However the sixfold exchange rate increase is twice the estimated threefold increase in solvent accessibility, implying a small effect of dissociation on helix stability.

H/D exchange rates for a membrane protein

It is of considerable interest to note how the rates observed compare with those previously observed in other proteins,

particularly membrane proteins and membrane-associated peptides. Previous work with membrane proteins has usually failed to assign exchange rates for the peptide groups in transmembrane helices with the exchange of these groups being very slow. The exceptions to this is the CHIP28 protein and the glucose transporter in which fast exchange (minutes) was observed and attributed to high water accessibility of these helices. We suspect that our observation of a slow but measurable exchange with a time constant of $\sim 6 \times 10^4$ min is aided by the use of a detergent-solubilized system rather than one embedded in a membrane and a system in which all the helices can be regarded as exterior to some extent. The precise effect of the lipid environment, detergent versus bilayer, and the bilayer phase remains to be clarified.

Above we assign an exchange with a time constant of between 100 and 25 min, depending on the dissociation state, to an amphipathic helix. Interestingly, previous measurements on phospholamban in dimyristoyl phosphatidyl choline bilayers (Ludlam et al., 1996) determined a time constant of ~500 min for the amide proton exchange of the amphipathic helix. This is slightly slower than the values that we determine here and attribute to an amphipathic helix but of a similar order of magnitude. Furthermore, the difference observed can be attributed almost exclusively to pH effects. Our measurements are at pH 8.0 as opposed to pH 7.4, which is expected to give a fourfold increase in the measured exchange rates. Any remaining difference in the time constants may well result from a small stabilization of this type of helix by phospholipid head groups or from differences in the helix lengths. The helix in the antenna complex is somewhat shorter than that in phospholamban. However, overall these very different amphipathic helices appear to have similar amide proton exchange rates and inference stabilities.

Implications for thermodynamics of membrane protein folding

We have observed above that the exchange rates of the amide nitrogens associated with the transmembrane helices of a membrane protein depend upon the degree of association of these helices. This effect probably is due to both an increase in the solvent accessibility and to dissociation-induced destabilization of the transmembrane helices. Interactions among secondary structure units stabilize these structural units is unsurprising. However, this is the first indication that this might be the case for transmembrane α-helices. This is of considerable interest for considerations of the thermodynamics of membrane protein assembly. According to the model of Popot and Engelman (1990), membrane protein folding and assembly in an initial series of step independently stable transmembrane helices are inserted into the membrane, and these subsequently pack with each other to form native multihelical membrane proteins. To date, very little information is available on the thermodynamics of the second of these stages, namely the packing of transmembrane helices. It is presumed that this step involves a positive entropic effect arising from the restriction of side chain motions compensated by enthalpic effects and possibly additional solvent entropic effects. Two of us measured a relatively large enthalpy change associated with one of the transitions in the system we study here, namely the formation of the tetrameric intermediate form (B820) from the fully dissociated form (B777) of -175 kJ mol^{-1} (Sturgis and Robert, 1994). However, to date estimations of the importance of the various assumed entropic effects in the aggregation of transmembrane helices are wanting. The results that we present here suggest that there is probably a small entropic effect opposing transmembrane helix aggregation in addition to the effect of side chain conformational restriction, namely the stabilization of the backbone conformation. This energetic component would result from the reduction in backbone conformational entropy visible as the inhibition of H/D exchange as a result of the association of transmembrane helices.

The results here show a progressive deprotection of the amide protons as the transmembrane helices of an integral membrane protein, the *R. rubrum* antenna complex, are dissociated. Such a deprotection would probably result on a molecular level from an increase in helix flexibility and, in particular, breathing motions necessary for proton exchange. This influence of helix packing on stability is probably larger in other more compact membrane proteins with a well defined interior than in the protein that we have studied, which lacks a well defined interior being toroidal.

REFERENCES

Alvarez, J., D. C. Lee, S. A. Baldwin, and D. Chapman. 1987. A Fourier transform infrared spectroscopy study of the structure and conformational changes of the human erythrocyte glucose transporter. *J. Biol. Chem.* 262:3502–3509.

Ashikawa, I, J. J. Yin, W. K. Subczynski, T. Kouyama, J. S. Hyde, and A. Kusumi. 1994. Molecular organization and dynamics on bacteriorhodopsin rich reconstituted membranes: discrimination of lipid environments by the oxygen transport parameter using a pulse ESR spin labeling technique. *Biochemisty*. 33:4947–4952.

Chang M. C., P. M. Callahan, P. S. Parkes-Loach, T. M. Cotton, and P. A. Loach. 1990. Spectroscopic characterization of the light-harvesting complex of *Rhodospirillum rubrum* and its structural subunit. *Biochemistry*. 29:421–429.

Cogdell, R. J., J. G. Lindsay, J. Valentine, and I. Durant. 1982. A further characterization of the B880 light harvesting pigment protein complex from *Rhodospirillum rubrum* strain S1. *FEBS Lett*. 150:151–154.

de Jongh H. H., E. Goormaghtigh, and J. M. Ruysschaert. 1996. The different molar absorptivities of the secondary structure types in the amide I region: an attenuated total reflection infrared study on globular proteins. *Anal. Biochem.* 242:95–103.

Earnest, T. N., J. Herzfeld, and K. J. Rothschild. 1990. Polarized Fourier transform infrared spectroscopy of bacteriorhodopsin: transmembrane alpha helices are resistant to hydrogen/deuterium exchange. *Biophys. J.* 58: 1539–1546.

Englander, S. W., and L. Mayne. 1993. Protein folding studied by using hydrogen-exchange labeling and two dimensional NMR. *Annu Rev. Biophys. Biomol. Struct.* 21:243–265.

Goormaghtigh E., V. Cabiaux, and J.-M. Ruysschaert. 1994a. Determination of soluble and membrane protein structure by Fourier transform

infrared spectroscopy. II. Experimental aspects, side chain structure, and H/D exchange. *Subcell. Biochem.* 23:363–403.

Goormaghtigh E., V. Cabiaux, and J.-M. Ruysschaert. 1994b. Determination of soluble and membrane protein structure by Fourier transform infrared spectroscopy. III. Secondary structures. *Subcell. Biochem.* 23: 405–450.

Goormaghtigh, E., and J.-M. Ruysschaert. 1994. Subtraction of atmospheric water contribution in Fourier transform infrared spectroscopy of biological membranes and proteins. *Spectrochim. Acta, Part A.* 50: 2137–2144.

Goormaghtigh, E., L. Vigneron, G. A. Scarborough, and J.-M. Ruysschaert. 1994c. Tertiary conformational changes of the neurospora crassa plasma membrane H^+-ATPase monitored by hydrogen/deuterium exchange kinetics. *J. Biol. Chem.* 269:27409–27413.

Haris, P. I., D. Chapman, and G. Benga. 1995. A Fourier transform infrared spectroscopic investigation of the hydrogen-deuterium exchange and secondary structure of the 20-kDa channel forming integral membrane protein (CHIP28) *Eur. J. Biochem.* 233:659–664.

Hu, X., T. Ritz, A. Damjanovic, and K. Schulten. 1997. Pigment organization and transfer of electronic excitation in purple bacteria. *J. Phys Chem.* 101: In press.

Janiak, M. J., D. M. Small, and G. G. Shipley. 1979. Temperature and compositional dependence of the structure of hydrated dimyristoyl lecithin. *J. Biol. Chem.* 254:6068–6078.

Karrasch S, P. A. Bullough, and R. Ghosh. 1995. The 8.5Å projection map of the light-harvesting complex I from Rhodospirillum rubrum reveals a ring composed of 16 subunits. *EMBO J.* 14:631–638.

Koepke J., X. Hu, C. Muenke, K. Schulten, and H. Michel. 1996. The crystal structure of the light-harvesting complex II (B800–850) of *Rhodospirillum molischianum. Structure (London)*. 4:581–597.

Loach, P. A., P. S. Parkes, J. F. Miller, S. Hinchigeri, and P. Callahan. 1985. Structure function relationships of the bacteriochlorophyll protein light-harvesting complex of *Rhodospirillum rubrum*. *In* Molecular Biology of the Photosynthetic Apparatus. C. Arntzen, L. Bogorad, S. Bonitz, and K. Steinback, editors. Cold Spring Harbor Laboratory Press, Cold Spring Harbor, NY. 197–209.

Ludlam, C. F. C., I. T. Arkin, X.-M. Liu, M. S. Rothman, P. Rath, S. Aimoto, S. O. Smith, D. M. Engelman, and K. J. Rothschild. 1996. Fourier transform infrared spectroscopy and site directed isotope labeling as a probe of local secondary structure in the transmembrane domain of phosopholamban. *Biophys. J.* 70:1727–1736.

McDermott G., S. M. Prince, A. A. Freer, A. M. Hawthornthwaite-Lawless, M.Z. Papiz, R. J. Cogdell, and N. W. Isaacs. 1995. Crystal structure of an integral membrane light-harvesting complex form photosynthetic bacteria. *Nature*. 374:517–521.

Olsen, J. D., J. N. Sturgis, G. Fowler, W. Westerhuis, C. N. Hunter, and B. Robert. 1997. Site-directed modification of the ligands to the bacteriochlorophylls of the light-harvesting LH1 and LH2 complexes of *Rhodobacter sphaeroides. Biochemistry*. 36:12625–12632.

Popot, J.-L., and D. Engelman. 1990. Membrane protein folding and oligomerization: the two stage model. *Biochemistry* 29:4031–4037.

Provencher S. W. 1982. A constrained regularization method for inverting data represented by linear algebraic or integral equations. *Computer Phys. Commun.* 27:213–227.

Raussens, V., V. Narayanaswami, E. Goormaghtigh, R. O. Ryan, and J.-M. Ruysschaert. 1996. Hydrogen/deuterium exchange kinetics of apolipophorin-III in lipid-free and phospholipid bound states: an analysis by Fourier transform infrared spectroscopy. *J. Biol. Chem.* 271: 23089–23095.

Sturgis, J. N., and B. Robert. 1995. A kinetic study of the reassociation of the antenna complex of *Rhodospirillum rubrum* in detergent solution. *In* Photosynthesis: From Light to Biosphere, Vol. 1. P. Mathis, editors. Kluwer Academic Publishers, Dordrecht. 255–258.

Sturgis, J. N., J. D. Olsen, B. Robert, and C. N. Hunter. 1997. The functions of conserved tryptophan residues of the core light harvesting complex of *Rhodobacter sphaeroides. Biochemistry* 36:2772–2778.

Sturgis, J. N., and B. Robert. 1994. Thermodynamics of membrane polypeptide oligomerization in light-harvesting complexes and associated structural changes. *J. Mol. Biol.* 238:445–454.